

Westerduinweg 3
1755 LE Petten
P.O. Box 15
1755 ZG Petten
The Netherlands

TNO report

TNO 2019 R11390

**Validation of BEM and Vortex-wake models with
full scale on-site measurements**

www.tno.nl

T +31 88 866 50 65

TKI WoZ VortexLoads WP3

Date	September 2019
Author(s)	K. Boorsma
Copy no	
No. of copies	
Number of pages	29 (incl. appendices)
Number of appendices	4
Sponsor	TKI WoZ
Project name	TKI WoZ VortexLoads
Project number	060.33833

All rights reserved.

No part of this publication may be reproduced and/or published by print, photoprint, microfilm or any other means without the previous written consent of TNO.

In case this report was drafted on instructions, the rights and obligations of contracting parties are subject to either the General Terms and Conditions for commissions to TNO, or the relevant agreement concluded between the contracting parties. Submitting the report for inspection to parties who have a direct interest is permitted.

© 2019 TNO

Acknowledgement

This project has been executed within the framework of TKI Wind op Zee.



Summary

Within the framework of the TKI WoZ VortexLoads project, a comparison was made between predicted and measured fatigue loads of a 2.5MW turbine at the EWTW test site. Over 7 years of measurements were analysed to obtain relevant statistics over 100.000 ten minute samples, of which about 25.000 remained after filtering out unwanted conditions (e.g. disturbed inflow). The data was bin averaged with respect to turbulence intensity and wind speed, after which dedicated simulations for each wind speed bin were ran at 10% turbulence intensity. The resulting load comparison shows BEM to over predict the fatigue equivalent flapwise blade root moments by approximately 15%, similar to a previous comparison against CFD within this project, where a vortex wake model comes closer to the measurements.

Care should be taken drawing conclusions on the basis of these results, since it is felt that comparing aero-elastic simulations to the used field data set is subject to many uncertainties (inflow, control, model data, compensating errors etc.) that cannot easily be verified. A great effort was made however to eradicate most of these, e.g. by running simulations for a large number of seeds and using a large number of measurement samples. It is recommended to set-up a dedicated field test in an effort to further reduce the underlying uncertainties. Here one can think of using nacelle LiDAR to characterize the inflow conditions in more detail for synthetic wind field creation in combination with pressure sensors to measure sectional aerodynamic loading.

Contents

	Summary	3
1	Introduction	5
2	Field test data	7
2.1	Description of set-up	7
2.2	Data reduction	7
2.3	Results	9
3	Comparison to simulations.....	10
3.1	Simulations	10
3.2	Comparison.....	11
4	Conclusions and Recommendations	12
5	References.....	13
	APPENDICES	15
A	Log of results from field data filtering	15
B	Field data plots	16
C	Turbsim example input	23
D	Comparison plots field data versus simulations	25

1 Introduction

The TKI WoZ VortexLoads project [1] considers the application of vortex wake models to design load calculations and its potential added value against traditional BEM methods. Within Work Package 3 of the project, validation of simulations against measurements is performed.

First initiatives to validate wind turbine aerodynamic modeling against measurements started in the eighties, where the EU project WTBE/ML project made a first effort towards validation of aero-elastic codes. Here measured and simulated blade root moments were compared and analysed. Soon it was realized that more detailed sectional load information was necessary for a better validation and understanding. IEA Wind Task 14 and 18 contributed to this objective where field measurements from all over the world (some including sectional pressure distributions) were studied by an international consortium of wind energy researchers [2, 3]. The main conclusion was that constant, uniform and controlled inflow conditions are necessary to make progress in this field, which led to a number of rotating wind tunnel experiments. The largest campaigns here are the NREL Phase VI measurements [4] and the (New) Mexico experiment [5, 6], which were analysed in IEA Task 20 [7] and 29 [8, 9, 10].

The results of these campaigns indicated that for uniform constant axial inflow, BEM and free vortex wake (FVW) codes are suitable to determine accurate performance and load level as long as the underlying airfoil data used by these codes is correct [10]. This is illustrated in Figure 1.1, which shows results grouped by code type versus the New Mexico experiment in axial (1.1(a)) and yawed inflow conditions (1.1(b)). It can also be observed that for this yawed flow condition, BEM methods fail to predict a good trend where vortex methods provide a better alternative.

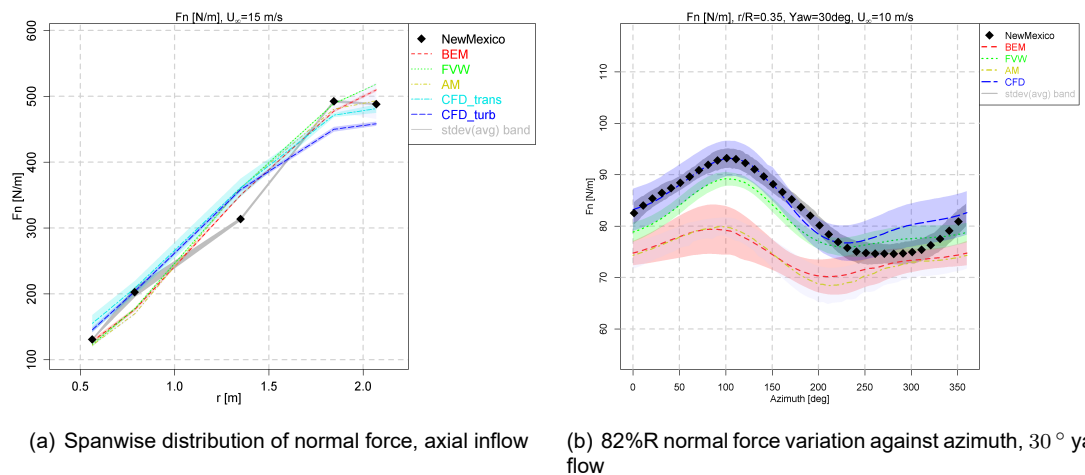


Figure 1.1: New Mexico measured normal force compared against grouped code type results from IEA Task 29 [10]

However wind tunnel measurements suffer from the fact that representative conditions for the field are difficult to match. An example is the absence of representative turbulent inflow conditions, which are subject of study in the TKI WoZ VortexLoads project. Over a decade of measurements on 2.5MW pitch to vane controlled research turbines is available from the EWTW test site of ECN part of TNO [11]. In an attempt to validate fatigue load predictions against field data, this database is used for a com-

parative study. This report presents the results of this study.

Chapter 2 describes the field test data used from the EWTW test site, its set-up and post-processing. Chapter 3 then describes the simulations and their comparison to the measured field test data, followed by conclusions and recommendations in Chapter 4.

2 Field test data

2.1 Description of set-up

The EWTW farm [12] that is subject of investigation consisted of a row of five 2500 kW turbines with variable speed-pitch regulated control. These turbines have a rotor diameter and hub height of 80 m and are placed at mutual distances of 3.8 rotor diameters (D). The farm is very well suited for investigation into effects at full scale because of its state of the art turbines and the comprehensive and reliable measurement infrastructure for turbine and meteorological data.

The farm was orientated from west to east ($95\text{-}275^\circ$), see Figure 2.1. Turbine 6 has been instrumented with blade root strain gauges and hence is used for the loads analysis. The wind characteristics are measured with the meteorological tower at $2.5D$ south-west of turbine 6. This mast measures wind speed and direction at three different heights including hub height. Also air pressure and temperature are measured at this height. More details can be found in the dedicated report [11]. The analyzed measurements at EWTW have been obtained from the period September 2004 until January 2012.

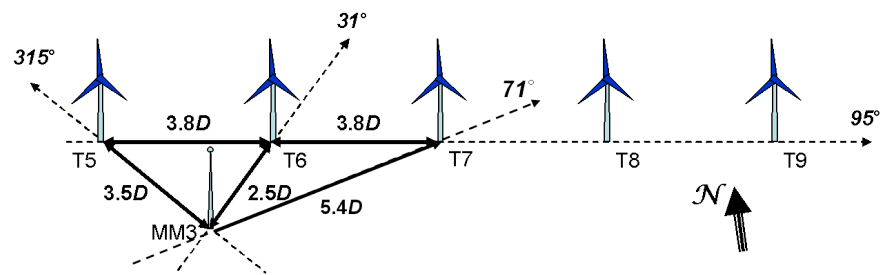


Figure 2.1: Main dimensions and directions in the EWTW farm. T5 to T9 are the turbine positions, MM3 indicates the measurement mast. Dimensions are expressed in rotor diameters D .

2.2 Data reduction

The SCADA and load signals of turbine 6 together with the meteorological data from mast 3 have been used for the analysis in this report. 10-minute statistics have been retrieved from the data base. A wind direction criterium based on the undisturbed wind sector (between $110\text{-}140^\circ$ and $200\text{-}250^\circ$) has been applied when retrieving the result from the database, resulting in about 100.000 ten minute samples.

2.2.1 Filtering

After retrieving the statistics from the database, a second data reduction step is performed to filter out erroneous samples and outliers. These steps are outlined below. For more details, please consult appendix A which contains a summary of the results of this procedure.

Non-numeric values In some cases a measurement signal is not recorded, e.g. due to a malfunction, resulting in a non-numeric value (NaN). The underlying ten minute samples are excluded from the dataset.

Power, operational mode Only normal operation conditions in power production are considered. Therefore the average power is filtered to be larger than 25 kW and the operational mode "op_mode" is restricted between 10.5 and 12.5.

Average wind speed Although operational mode and minimum power filters should have excluded unsuitable samples, the average wind speed has also been restricted between 4.5 and 15.5 m/s.

Nacelle direction standard deviation The standard deviation of the nacelle direction indicates to what extent the turbine has been yawing during the sample. Samples have been excluded for standard deviation exceeding 15° .

Nacelle to wind speed ratio The wind speed is measured at the meteo mast located 3.5 diameters distance from the turbine. There can be differences between the wind that is experienced by the turbine and the meteo mast. Since the wind speed at the meteo mast is used to correlate with the turbine measurements, the ratio between average meteo mast and nacelle wind speed is restricted to values above 0.85.

Wind shear Samples which feature a too high or low vertical shear are omitted by observing the ratio between measured wind speed at 80 m and 50 m. The ratio between the two is restricted between 1.0 and 1.2.

Turbine misalignment The turbine misalignment is determined by subtracting averaged wind direction from nacelle direction. This value is restricted between -20° and 12.5° . The asymmetry in this filter was proposed because of previously observed misalignment of this turbine [13].

Turbulence intensity The turbulence intensity can be calculated by dividing the standard deviation of the wind speed over its average, both measured at the meteo mast. Extremely low and high values are filtered out by restricting this value between 2.5% and 27.5%

Pitch angle variation To limit the amount of pitch action within a data point, the difference between the maximum and minimum pitch angle of a data set is restricted to 0.2° . This requirement effectively filters out above rated data points, where pitching action is common.

Starting with about 100.000 ten minute samples from the database, about 25.000 remained after the above specified filtering (see also appendix A).

2.2.2 *Correction for atmospheric conditions*

Power, edgewise and flatwise moments scale different with atmospheric conditions. The edgewise moment is dictated by gravity forces and the flatwise moment by aerodynamic force. The latter is influenced by atmosphere linearly through air density. The variation of the air density can be shown to lie between 1.20 and 1.26 kgm^{-3} for the selected samples. This is regarded as a small variation and hence the influence of atmospheric conditions is not taken into account.

2.2.3 *Fatigue equivalent moments*

The fatigue equivalent flatwise and edgewise moments of turbine 6 are acquired for for a slope of 10 (glass fibre). The rain-flow counting method was applied to the raw signal and the equivalent loads have readily been determined in the database according to IEC 61400-13 [14].

2.2.4 Bin averaging

Bin averaging is applied to the resulting data sets both in wind speed and turbulence intensity. The bin averaging settings are given in Table 2.1. The standard error of the mean within each bin is calculated using

$$S = \sigma / \sqrt{N} \quad , \quad (2.1)$$

with

- S [] standard error of bin average mean
- σ [] standard deviation of the bin data samples
- N [-] number of samples per bin.

Table 2.1: Bin averaging settings

Required samples per bin for valid average	6
Wind speed bins	5 to 13 m/s, $\Delta = 1$ m/s
Turbulence intensity bins	5% to 20%, $\Delta = 2.5\%$

2.3 Results

The resulting dataset from the filtering and binning has been visualized using contour plots as a function of turbulence intensity and wind speed. The plots are given in appendix B. From Figure B.1 it can be observed that although average values of flap and edgewise moments are relatively insensitive to variation of turbulence intensity, a clear trend with this variable can be observed for the fatigue equivalent (here it is noted that flap- and flatwise blade root moment are the same for a pitch angle for zero degree). For the standard deviation of the flatwise moment a similar trend can be observed. The gradient with turbulence intensity for the standard deviation of the edgewise moment seems more steep in comparison to this gradient for the fatigue equivalent edgewise moment. Figure B.2 indicates there is hardly any difference between the three blades. Although the range values are not shown here, they are highly similar, especially for the flatwise moments. Figure B.3 shows most of the samples are centered around 8% turbulence intensity between 6 and 11 m/s. The average yaw misalignment angle is small and centered around -3° . As indicated above the air density variation is minimal. Although the average of the rotor speed in Figure B.4 features only a small influence of turbulence intensity at the highest levels, the rotor speed dynamics (in terms of minimum, maximum and standard deviation) is clearly affected as expected. Although the turbine is operating below rated wind speed (12 m/s) for the resulting dataset, the pitch angles in Figure B.5 are not averaging to zero but show an average value of around 0.15° , similar between the three blades. The standard error as defined in equation 2.1 is visualized in Figure B.6 for the blade root moments. Although the values of the blade root moments were not given in the previously discussed Figures, the standard error is mostly less than 1% of these moments. This is a consequence of the high number of 10 minute samples, especially for turbulence intensities below 12%.

3 Comparison to simulations

Using the bin averaged operational conditions from the field data analysis, simulations are performed for all wind speed bins (5 to 12 m/s) focusing at the 10% turbulence intensity bin. The simulations and their set-up are discussed first, after which a comparison is made against the field data that was presented in section 2.

3.1 Simulations

A full aero-elastic model of the 2.5MW research turbine was built using Phatas [15] as embedded in the FOCUS6 software [16], including mass, stiffness, control and aerodynamic details as disclosed by the manufacturer. In order to create a representative value for the fatigue loads, six ten minute seeds were created per wind speed bin using the Turbsim wind generator [17], making sure that the resulting turbulence intensity matched the specification from the field data analysis. An example of the input file to the Turbsim generator is included in appendix C. For the evaluation of rotor aerodynamics the FOCUS6 software includes a coupling to the ECN Aero Module [18, 19]. The two aerodynamic models included herein are the Blade Element Momentum (BEM) method similar to the implementation in Phatas [15] and a free vortex wake code in the form of AWSM [20]. Both models are lifting line codes, i.e. they make use of aerodynamic look-up tables to evaluate airfoil performance. Several dynamic stall models, 3D correction models, wind modeling options and a module for calculating tower effects are included. The set-up allows to easily switch between the two aerodynamic models whilst keeping the external input the same, which is a prerequisite for a good comparison between them. The time increment was fixed to 0.02s.

For the BEM simulations, default options have been used unless mentioned otherwise. Simulation have been performed with both the Snel dynamic stall model [21] (PhatAero-BEM) and the Beddoes Leishman model [22] (PhatAero-BEM-BL, i.e. BEM only) to shed some light on the influence of shed vorticity modeling. Rotational corrections were enabled using the Snel method [23]. The simulations were ran with the controller activated, resulting in rotational speed variations over each the ten minute simulation. The yaw angle was set to the average value from the field data analysis.

In view of the limited time, the amount of AWSM simulations (PhatAero-AWSM) was limited to only a few seeds. For each wind speed considered, a representative seed was selected which matched the statistics and equivalent loads compared to the average over the six seeds for each wind speed bin as good as possible. For these representative seeds, the rotational speed variations resulting from the BEM simulations were recorded and fed to the AWSM simulations to have a consistent comparison between them. Similar to the BEM simulations, the Snel dynamic stall [21] and rotational correction model [23] were enabled. The statistics and equivalent loading of all simulation results were obtained after skipping the first 100 seconds, which is regarded as initialisation time, hence using the remaining 500 seconds.

For the free vortex wake simulation, the number of wake points was chosen to make sure that the wake length was developed over at least three rotor diameters downstream of the rotor plane. The wake convection was free for the first part (two diameters downwind of the rotorplane) of the wake. For the remaining wake length, the blade averaged induction at the free to fixed wake transition is applied to all wake points. For the AWSM simulations, wake reduction [24] was applied after approximately half a diameter of convected wake, skipping shed vortices to end up with an

effective distance of 10° azimuth between the shed vortices in the remaining part of the wake.

3.2 Comparison

Similar to the binning of the measured 10 minute statistics, the simulation results were averaged over the six available seeds for each wind speed bin. In addition to that also the standard error was calculated in accordance with equation 2.1. The resulting comparison plots are given in Appendix D. The results for the elected representative seeds as described in section 3.1 are also given indicated by PhatAero-BEM-seeds and PhatAero-AWSM-seeds. From Figure D.1 it can be observed that the resulting rotor speeds from the controller agree well with the field data, although the standard deviation indicates that the simulations feature more rotor speed variation than the measurements. Although the selected wind speeds are below rated, the measured pitch angle shows an offset compared to the simulations. Judging by its standard deviation some pitching action (although very small) has been measured in the field, not present in the simulations. The resulting power levels are consistent between measurements and predictions. The power values have been non-dimensionalized using the average of the field data results over the wind speed bins. The same holds for the blade root moments as displayed in Figure D.2 to D.4. The averaged edgewise moment are under predicted by the simulations. It is noted that the edgewise moments are dominated by gravitational variation, which makes it hard to determine the average levels with significant accuracy in the field. It is then assuring to observe the standard deviation and fatigue equivalents of the edgewise moments are in good agreement between simulations and measurements.

The averaged flatwise moments are slightly (<5%) underpredicted by the simulations, where they agree well between the different simulation settings. The equivalent loading and standard deviation for the flatwise moments are over predicted around 15% by the BEM simulations (averaged over all seeds and blades), where the AWSM vortex wake simulations are very close to the measurements (-1% averaged over all seeds and blades). This trend is similar to the results obtained from the comparison to CFD [25]. It is noted that the rainflow counting procedure to determine fatigue loads is insensitive to an offset in the average levels, as it is the magnitude or range of the fluctuations that matter.

Zooming in further on the fatigue load differences for the flatwise moments, we can observe the absolute difference between measurements and BEM simulations to increase with wind speed. However the relative difference in terms of percentage remains largely constant over the wind speed range. Application of the Beddoes Leishman model (PhatAero-BEM-BL), which adds modeling of shed vorticity effects, reduces the difference with the measurements only slightly (around 1% decrease). This is not in agreement with the comparison to CFD featuring the 10MW AVATAR rotor [25], which showed the modeling of shed vorticity to reduce the difference between BEM and high fidelity models significantly. It is unclear at this point what is causing the discrepancy between these observations.

4 Conclusions and Recommendations

A comparison was made between predicted and measured fatigue loads of a real turbine at the EWTW test site. Over 7 years of measurements were analysed to obtain relevant statistics over 100.000 ten minute samples, of which about 25.000 remained after filtering out unwanted conditions. The data was bin averaged with respect to turbulence intensity and wind speed, after which dedicated simulations for each wind speed bin were ran at 10% turbulence intensity. The resulting load comparison shows BEM to over predict the fatigue equivalent flapwise blade root moment by approximately 15%, similar to the comparison against CFD, where a vortex wake model comes closer to the measurements.

Care should be taken drawing conclusions on the basis of these results, since it is felt that comparing aero-elastic simulations to field data is subject to many uncertainties (inflow, control, model data, compensating errors etc.) that cannot easily be verified. A great effort was made however to eradicate most of these, e.g. by running simulations for a large number of seeds and using a large number of measurement samples. It is recommended to set-up a dedicated field test in an effort to further reduce the underlying uncertainties. Here one can think of using nacelle LiDAR to characterize the inflow conditions in more detail for synthetic wind field creation in combination with unsteady pressure sensors to measure sectional aerodynamic loading. In addition to that it is recommended to include more vortex wake simulations (similar to the number of BEM simulations) to better quantify the difference between these code types.

5 References

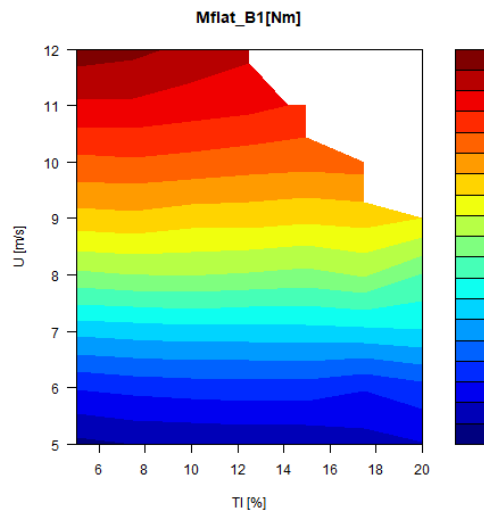
- [1] K. Boorsma and F. Wenz and M. Aman and C. Lindenburg and M. Kloosterman. TKI WoZ VortexLoads Final report. Technical Report TNO 2019 R11388, TNO, September 2019. <http://publications.tno.nl/publication/34634923/tbIASC/TNO-2019-R11388.pdf>.
- [2] J.G. Schepers, A. Brand, A. Bruining, J. Graham, M. Hand, D. Infield, H. Madsen, J. Paynter, and D. Simms. Final Report of IEA Annex XIV: Field Rotor Aerodynamics. Technical report, ECN-C-97-027, 1997.
- [3] J.G. Schepers et al. Final report of IEA Annex XVIII' Enhanced Field Rotor Aerodynamics Database. ECN-C-02-016, Energy Research Centre of the Netherlands, ECN, February 2002.
- [4] M.M. Hand, D.A. Simms, L.J. Fingersh, D.W. Jager, J.R. Cotrell, S. Schreck, and S.M. Larwood. Unsteady Aerodynamics Experiment Phase VI Wind Tunnel Test Configurations and Available Data Campaigns. NREL/TP-500-29955, National Renewable Energy Laboratory, NREL, December 2001.
- [5] J.G. Schepers and H. Snel. MEXICO, Model experiments in controlled conditions. ECN-E-07-042, Energy Research Center of the Netherlands, 2007.
- [6] K. Boorsma and J.G. Schepers. In *Rotor experiments in controlled conditions continued: New Mexico*, Proceedings of the Science of Making Torque from Wind, Technical University of Munich, 2016.
- [7] S. Schreck. IEA Wind Annex XX: HAWT Aerodynamics and Models from Wind Tunnel Measurements. NREL/TP-500-43508, The National Renewable Energy Laboratory, NREL, December 2008.
- [8] J.G. Schepers and K. Boorsma et al. Final report of IEA Task 29, Mexnext (Phase 1): Analysis of MEXICO wind tunnel measurements. ECN-E-12-004, Energy Research Center of the Netherlands, February 2012.
- [9] J.G. Schepers and K. Boorsma et al. Final report of IEA Task 29, Mexnext (Phase 2). ECN-E-14-060, Energy Research Center of the Netherlands, December 2014.
- [10] K. Boorsma and J.G. Schepers et al. Final report of IEA Task 29, Mexnext (Phase 3). ECN-E-18-003, Energy Research Center of the Netherlands, January 2018.
- [11] Machielse, L.A.H. Validatiemetingen EWTW, Eindrapport. Technical Report ECN-E-06-062, ECN, 2006.
- [12] P.J. Eecen et al. Measurements at the ECN wind turbine test station wieringermeer. Technical Report ECN-RX-06-055, ECN, 2006.
- [13] Boorsma, K. Power and loads for wind turbines in yawed conditions, Analysis of field measurements and aerodynamic predictions. Technical Report ECN-C-12-047, ECN, 2012.
- [14] IEC TS 61400-13, Wind turbine generator systems Part 13: Measurement of mechanical loads, June 2001.
- [15] C. Lindenburg and J.G. Schepers. Phatas-iv aeroelastic modelling, release "dec-1999" and "nov-2000". Technical Report ECN-CX-00-027, ECN, 2000.
- [16] <http://www.wmc.eu/focus6.php>. 2016.

- [17] B.J. Jonkman and M.L. Buhl, Jr. TurbSim User's Guide. NREL/TP-500-39797, National Renewable Energy Laboratory, NREL, September 2006.
- [18] K. Boorsma, F. Grasso, and J.G. Holierhoek. Enhanced approach for simulation of rotor aerodynamic loads. Technical Report ECN-M-12-003, ECN, presented at EWEA Offshore 2011, Amsterdam, 29 November 2011 - 1 December 2011, 2011.
- [19] K. Boorsma, M. Hartvelt, and L.M. Orsi. Application of the lifting line vortex wake method to dynamic load case simulations. *Journal of Physics: Conference Series*, 753(2):022030, 2016.
- [20] A. Van Garrel. Development of a wind turbine aerodynamics simulation module. Technical Report ECN-C-03-079, ECN, 2003.
- [21] H. Snel. Heuristic modelling of dynamic stall characteristics. In *Conference proceedings European Wind Energy Conference*, pages 429–433, Dublin, Ireland, October 1997.
- [22] J Gordon Leishman and TS Beddoes. A semi-empirical model for dynamic stall. *Journal of the American Helicopter society*, 34(3):3–17, 1989.
- [23] H. Snel, R. Houwink, J. Bosschers, W.J. Piers, G.J.W. van Bussel, and A. Bruining. Sectional prediction of 3-D effects for stalled flow on rotating blades and comparison with measurements. In *Proceedings of the European Community Wind Energy Conference*, 1993.
- [24] K. Boorsma, L. Greco, and G. Bedon. Rotor wake engineering models for aeroelastic applications. *Journal of Physics: Conference Series*, 1037(6):062013, 2018.
- [25] K. Boorsma and M. Aman and C. Lindenburg and F. Wenz. Validation of BEM and Vortex-wake models with numerical tunnel data, TKI WoZ Vortexloads WP2. Technical Report TNO 2019 R11389, TNO, September 2019. <http://publications.tno.nl/publication/34634924/jVk0uF/TNO-2019-R11389.pdf>.

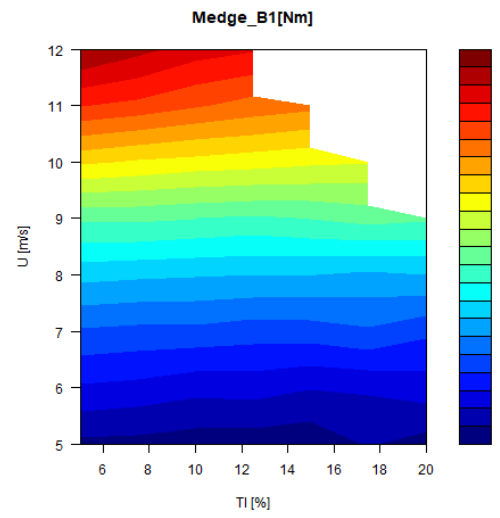
A Log of results from field data filtering

```
"start length:100910"  
"NaN in yaw_T6:4983"  
"NaN in MM3_WS80_240_avg: 163"  
"NaN in MM3_WS80_240_std: 0"  
"NaN in MM3_Pair80_avg: 1057"  
"NaN in T6_Popmode_avg: 5"  
"NaN in T6_Mbf1_load_P_avg: 20439"  
"NaN in T6_Mbf2_load_P_avg: 8780"  
"NaN in T6_Mbf3_load_P_avg: 6189"  
"NaN in T6_Mbe1_load_P_eql_m10: 3452"  
"NaN in T6_Mbe2_load_P_eql_m10: 0"  
"NaN in T6_Mbe3_load_P_eql_m10: 0"  
"NaN in T6_Mbf1_load_P_eql_m10: 0"  
"NaN in T6_Mbf2_load_P_eql_m10: 0"  
"NaN in T6_Mbf3_load_P_eql_m10: 0"  
"NaN in T6_Rspd_avg: 321"  
"NaN in T6_Ppitch1_avg: 151"  
"NaN in T6_Ppitch2_avg: 226"  
"NaN in T6_Ppitch3_avg: 52"  
"NaN in T6_PEpow_avg: 0"  
"power T6>25:8679"  
"op_mode (10.5 to 12.5) :417"  
"nacelle dir std T6 (<15) :25"  
"windspeed (4.5 to 15.5 m/s) :4276"  
"v/v_nac T6 (>0.85) :179"  
"TI (0.025 to 0.275) :1893"  
"pitch_dif T6 (<0.2 deg) :7422"  
"wind shear ws80/ws50 (1 to 1.2 ):6469"  
"Misalignment T6 (-20 to 12.5 ):0"  
"Remaining nr of samples: 25732"
```

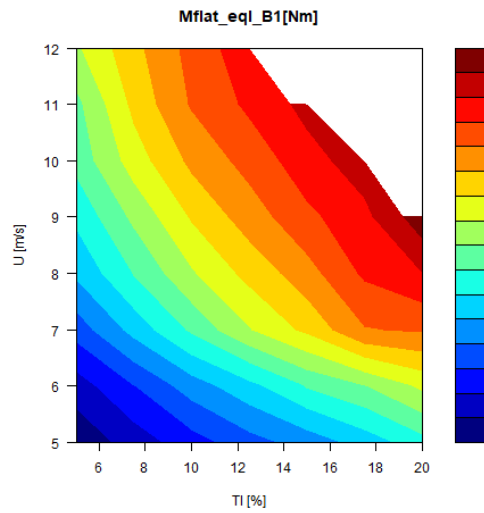
B Field data plots



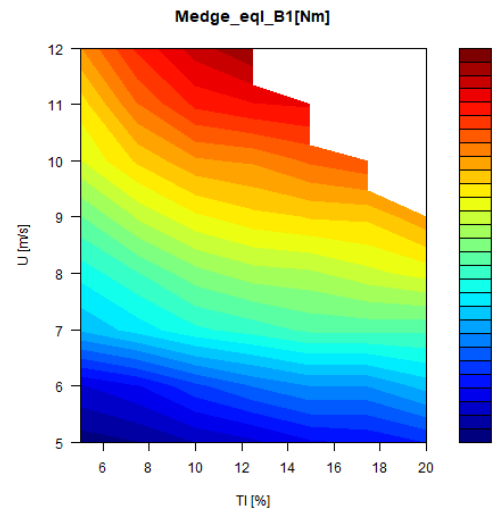
(a) Flatwise moment avg, blade 1



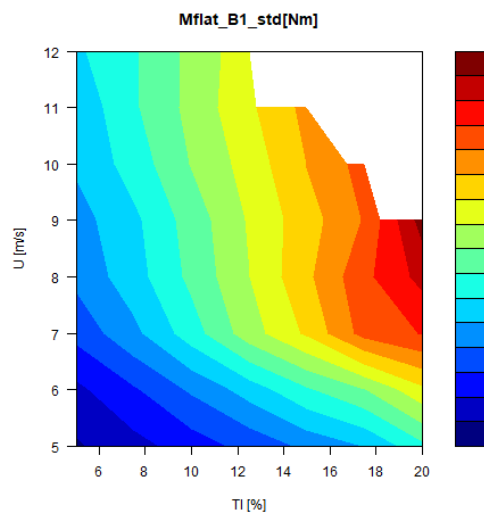
(b) Edgewise moment avg, blade 1



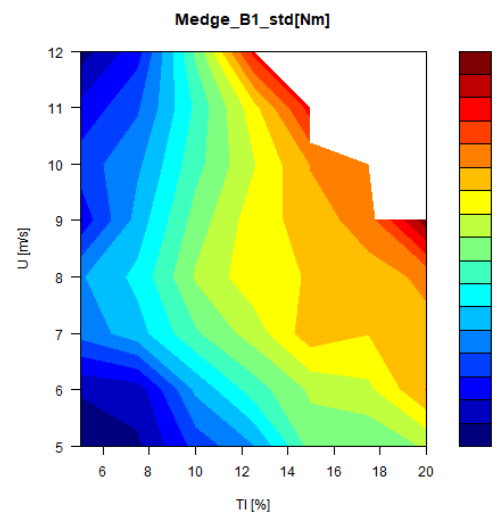
(c) Flatwise moment eq1, blade 1



(d) Edgewise moment eq1, blade 1

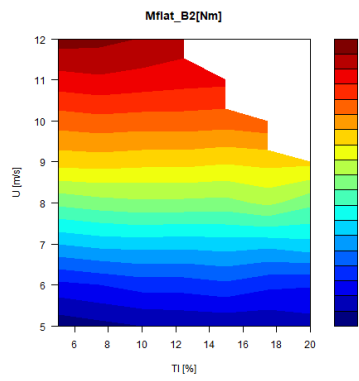


(e) Flatwise moment std, blade 1

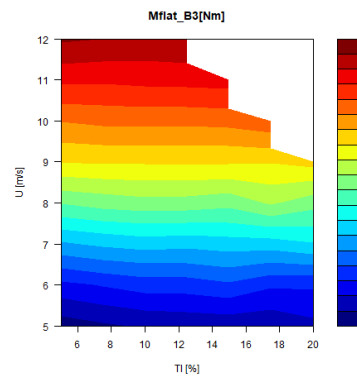


(f) Edgewise moment std, blade 1

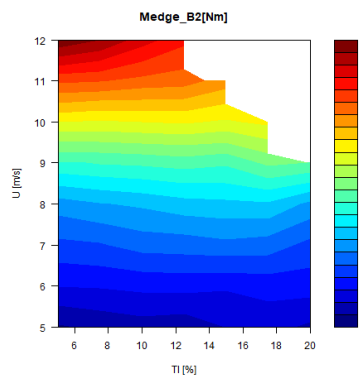
Figure B.1: Visualization of resulting field data (1)



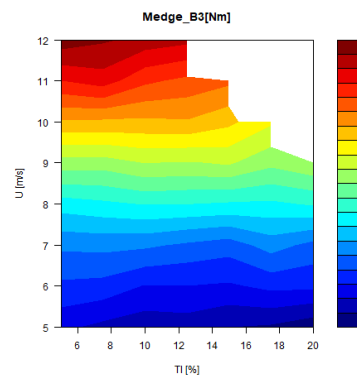
(a) Flatwise moment avg, blade 2



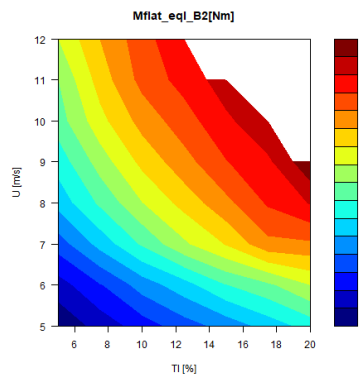
(b) Flatwise moment avg, blade 3



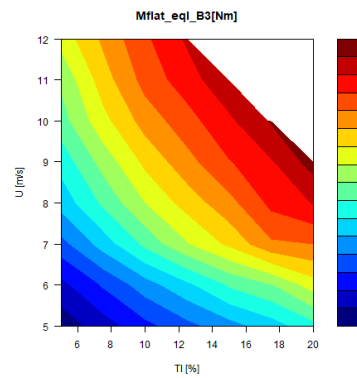
(c) Edgewise moment avg, blade 2



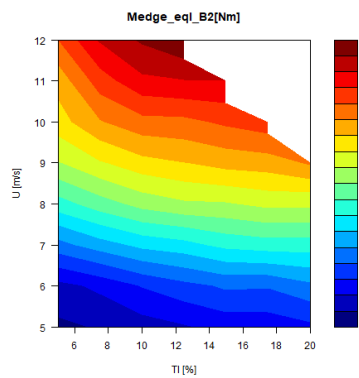
(d) Edgewise moment avg, blade 3



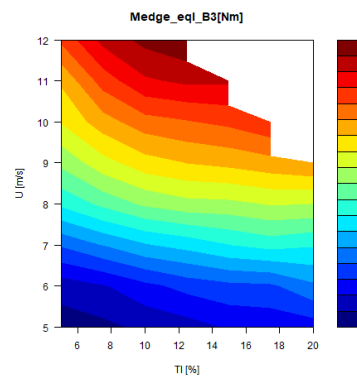
(e) Flatwise moment eq1, blade 2



(f) Flatwise moment eq1, blade 3



(g) Edgewise moment eq1, blade 2



(h) Edgewise moment eq1, blade 3

Figure B.2: Visualization of resulting field data (2)

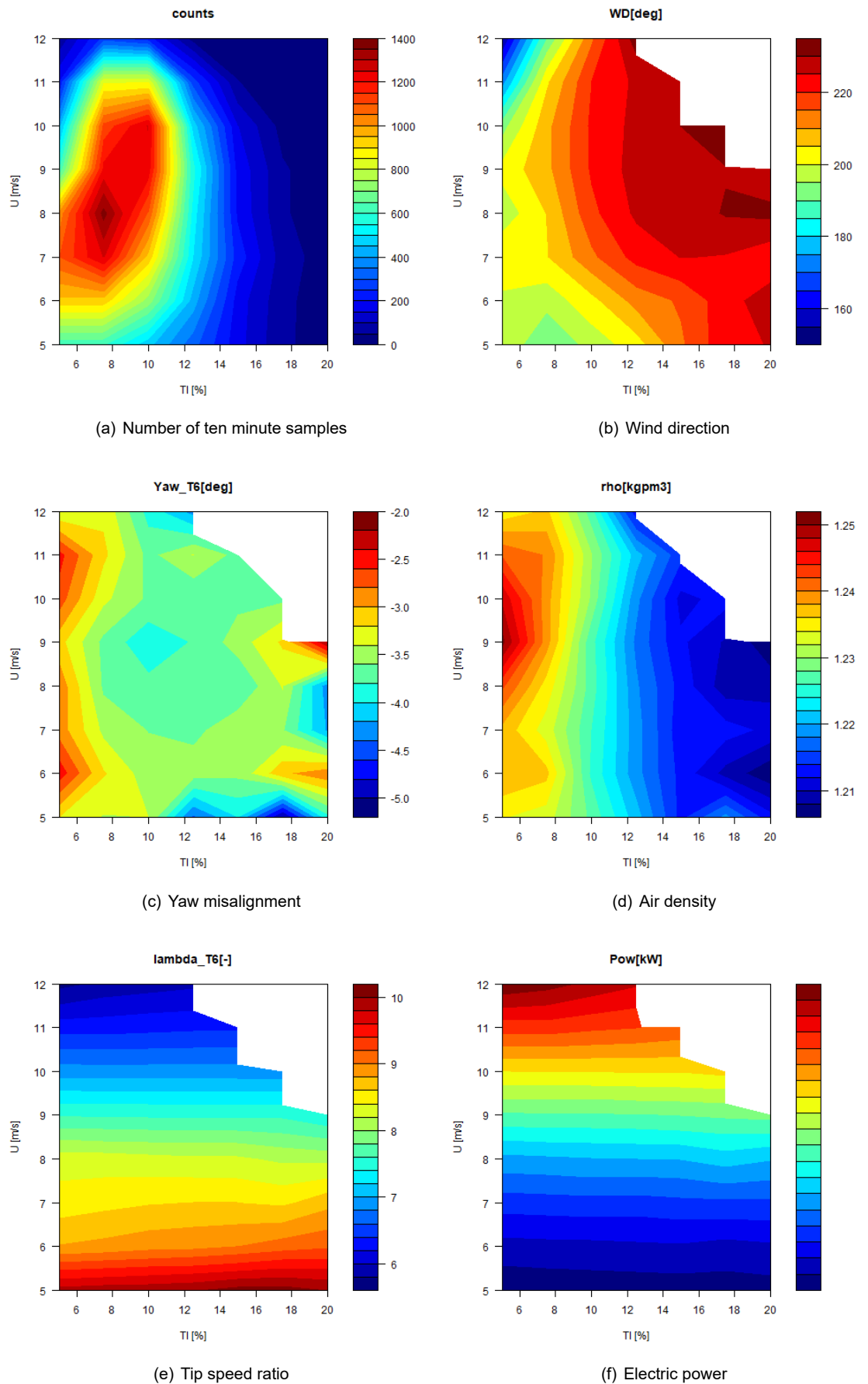


Figure B.3: Visualization of resulting field data (3)

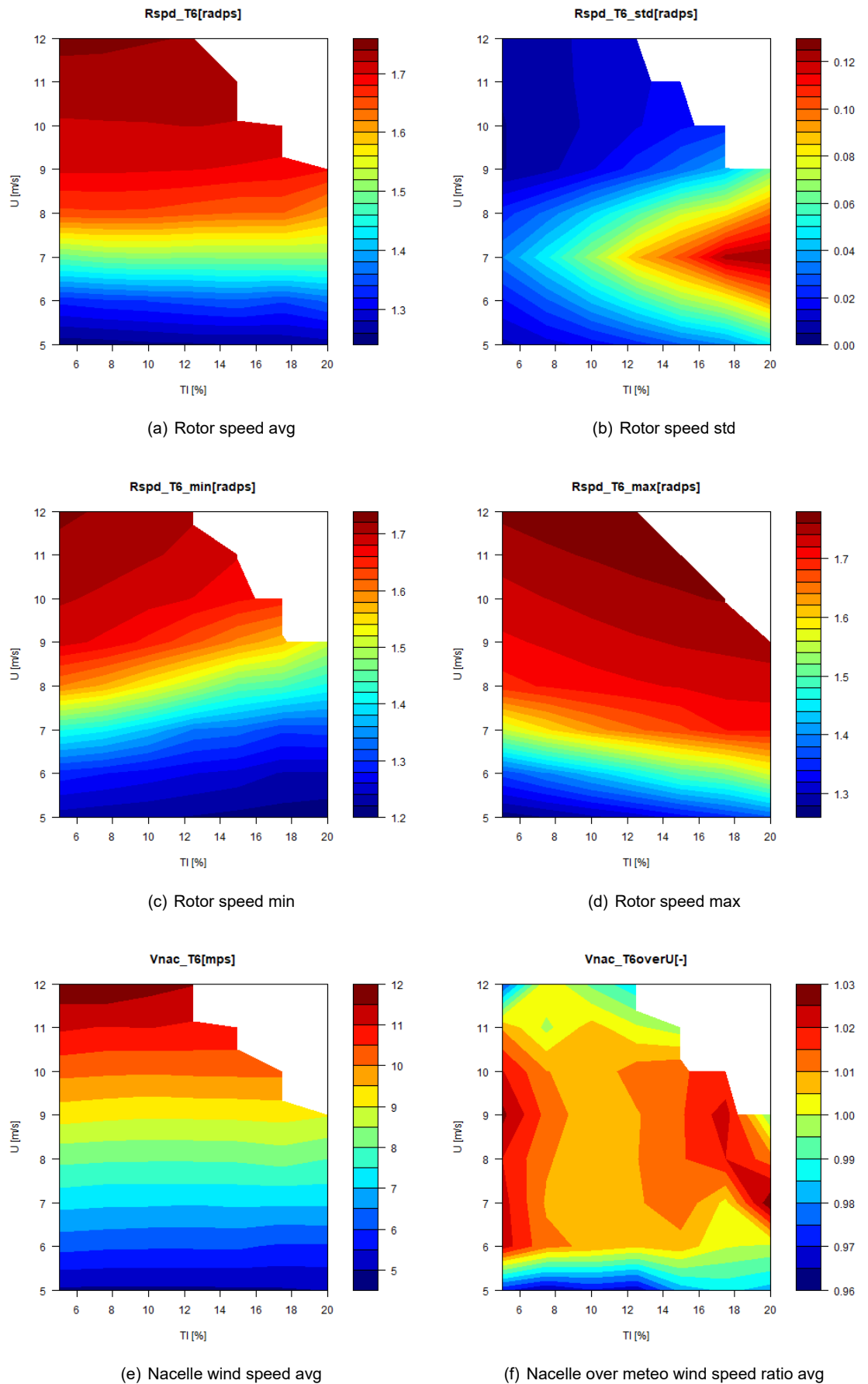
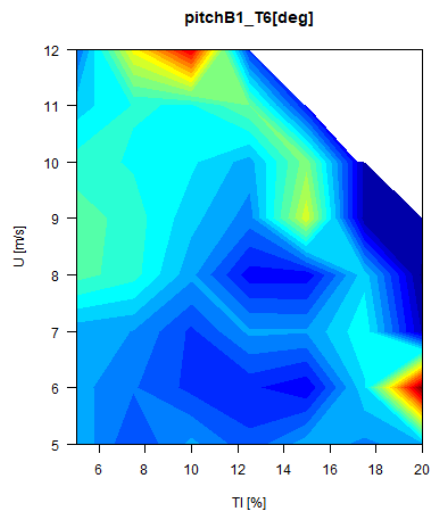
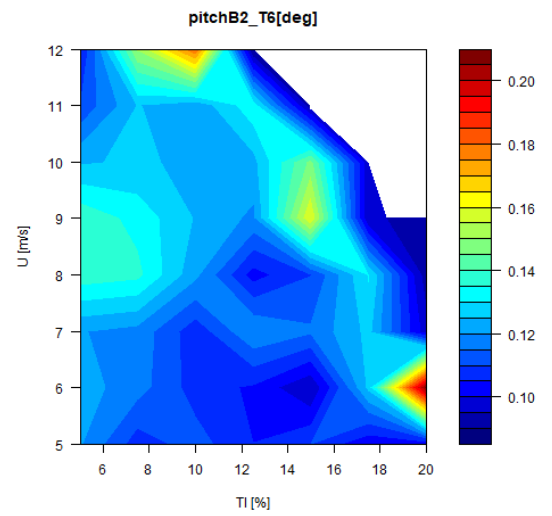


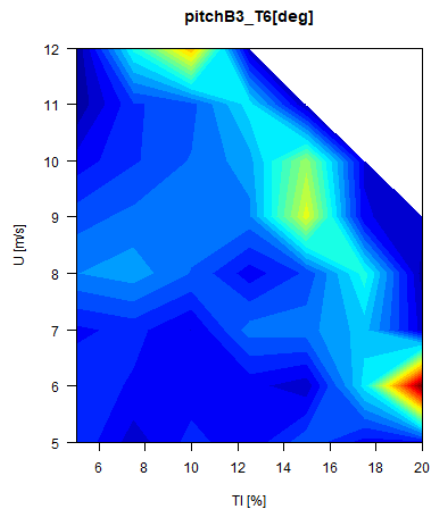
Figure B.4: Visualization of resulting field data (4)



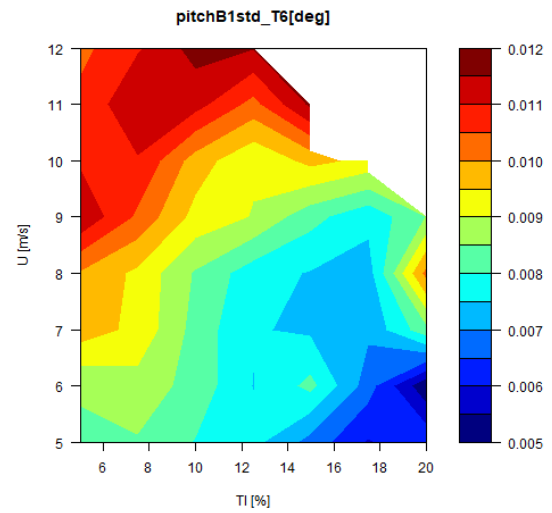
(a) Pitch angle avg, blade 1



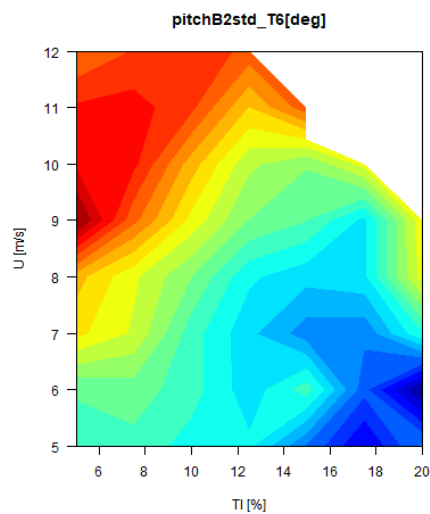
(b) Pitch angle avg, blade 2



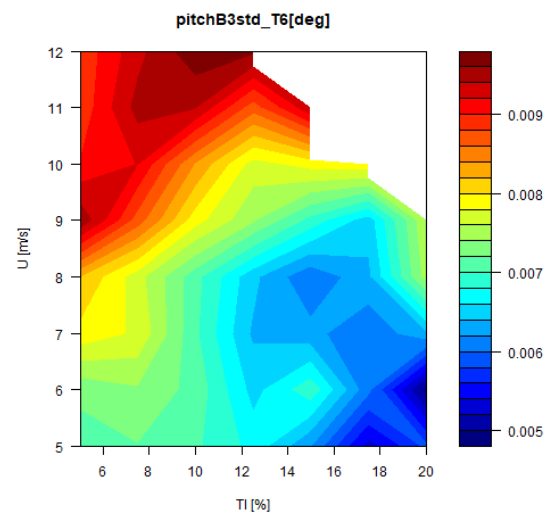
(c) Pitch angle avg, blade 3



(d) Pitch angle std, blade 1



(e) Pitch angle std, blade 2



(f) Pitch angle std, blade 3

Figure B.5: Visualization of resulting field data (5)

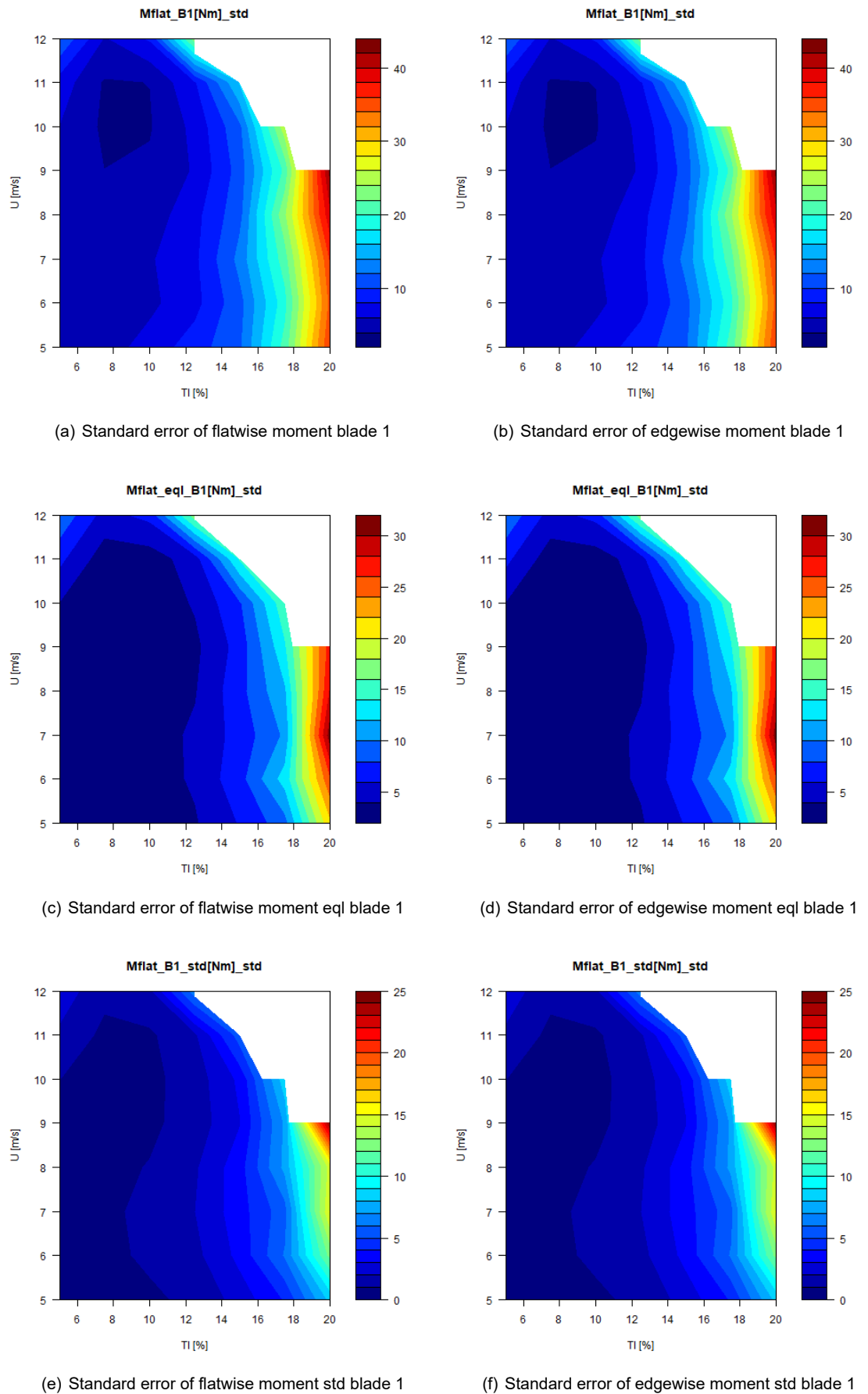


Figure B.6: Visualization of resulting field data (6)

C Turbsim example input

TurbSim Input File for 8m/s seed 1. Valid for TurbSim v1.06.00, 21-Sep-2012

```

-----Runtime Options-----
1          RandSeed1      - First random seed (-2147483648 to 2147483647)
RANLUX    RandSeed2      - Second random seed (-2147483648 to 2147483647)
False     WrBHHTP        - Output hub-height turbulence parameters in binary form?
True      WrFHHTP        - Output hub-height turbulence parameters in formatted form?
False     WrADHH         - Output hub-height time-series data in AeroDyn form?
False     WrADFF         - Output full-field time-series data in TurbSim/AeroDyn form?
True      WrBLFF         - Output full-field time-series data in BLADED/AeroDyn form?
False     WrADTWR        - Output tower time-series data? (Generates RootName.twr)
False     WrFMTFF        - Output full-field time-series data in formatted (readable) form?
False     WrACT          - Output coherent turbulence time steps in AeroDyn form?
True      Clockwise      - Clockwise rotation looking downwind?
1         ScaleIEC       - Scale IEC turbulence models to exact target standard deviation?

-----Turbine/Model Specifications-----
20         NumGrid_Z      - Vertical grid-point matrix dimension
20         NumGrid_Y      - Horizontal grid-point matrix dimension
0.01      TimeStep       - Time step [seconds]
600       AnalysisTime   - Length of analysis time series [seconds]
600       UsableTime     - Usable length of output time series [seconds]
80        HubHt         - Hub height [m] (should be > 0.5*GridHeight)
90.00     GridHeight     - Grid height [m]
90.00     GridWidth      - Grid width [m] (should be >= 2*(RotorRadius+ShaftLength))
0         VFlowAng       - Vertical mean flow (uptilt) angle [degrees]
0         HFlowAng       - Horizontal mean flow (skew) angle [degrees]

-----Meteorological Boundary Conditions-----
"IECKAI"  TurbModel      - Turbulence model ("IECKAI"=Kaimal, "IECVKM"=von Karman)
"1-ED3"   IECstandard    - Number of IEC 61400-x standard
9.88339891568233 IECturbc    - IEC turbulence characteristic
"NTM"     IEC_WindType   - IEC turbulence type
default   ETMc           - IEC Extreme Turbulence Model "c" parameter [m/s]
default   WindProfileType - Wind profile type
80        RefHt          - Height of the reference wind speed [m]
8.01334015510949 URef          - Mean (total) wind speed at the reference height [m/s]
default   ZJetMax        - Jet height [m] (used only for JET wind profile, valid 70-490 m)
default   PLExp          - Power law exponent [-] (or "default")
default   Z0             - Surface roughness length [m] (or "default")

-----Non-IEC Meteorological Boundary Conditions-----
default   Latitude       - Site latitude [degrees] (or "default")
0.05     RICH_NO         - Gradient Richardson number
default   UStar          - Friction or shear velocity [m/s] (or "default")
default   ZI             - Mixing layer depth [m] (or "default")
default   PC_UW          - Hub mean u'w' Reynolds stress (or "default")
default   PC_UV          - Hub mean u'v' Reynolds stress (or "default")
default   PC_VW          - Hub mean v'w' Reynolds stress (or "default")
default   IncDec1        - u-component coherence parameters
default   IncDec2        - v-component coherence parameters
default   IncDec3        - w-component coherence parameters

```

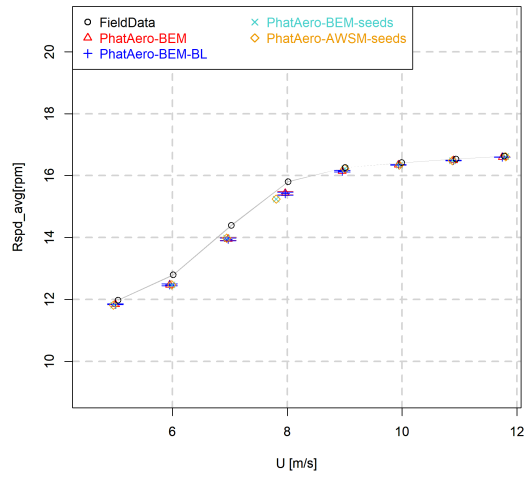
default CohExp - Coherence exponent (or "default")

-----Coherent Turbulence Scaling Parameters-----

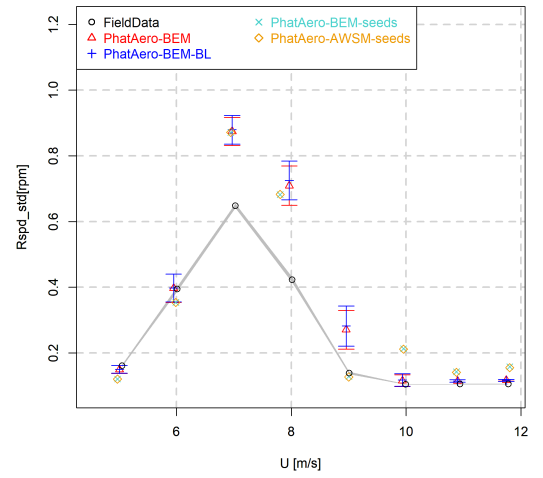
default CTEventPath - Name of the path where event data files are located
 "Random" CTEventFile - Type of event files ("LES", "DNS", or "RANDOM")
 true Randomize - Randomize the disturbance scale and locations? (true/false)
 1.0 DistSc1 - Disturbance scale
 0.5 CTly - Fractional location of tower centerline from right
 0.5 CTLz - Fractional location of hub height from the bottom of the dataset.
 30.0 CTStartTime - Minimum start time for coherent structures in RootName.cts

=====
 NOTE: Do not add or remove any lines in this file!
 =====

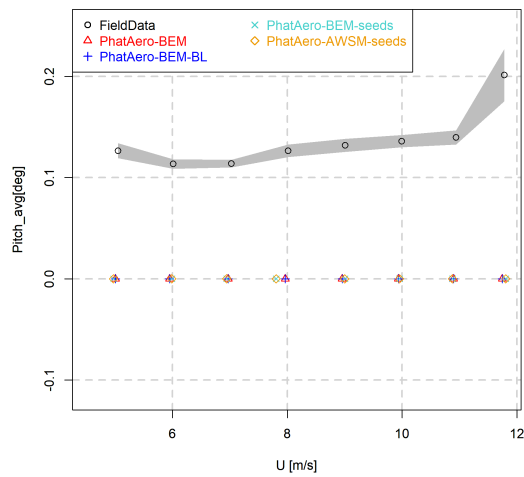
D Comparison plots field data versus simulations



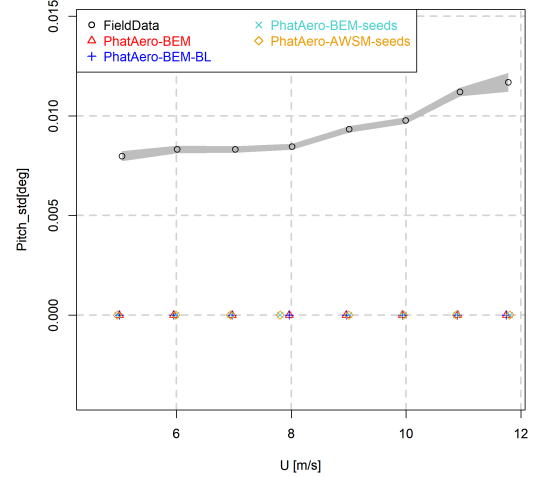
(a) Rotor speed average



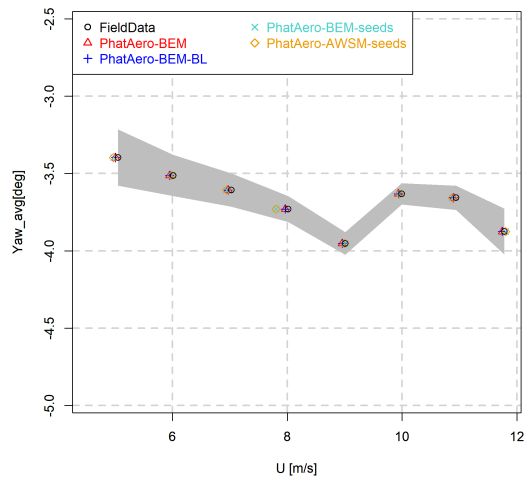
(b) Rotor speed standard deviation



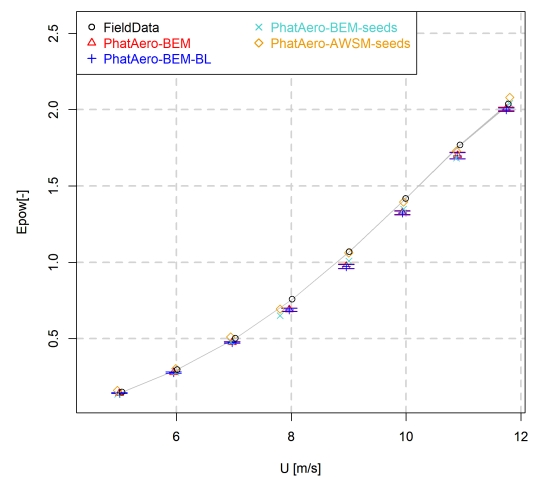
(c) Pitch angle average blade 1



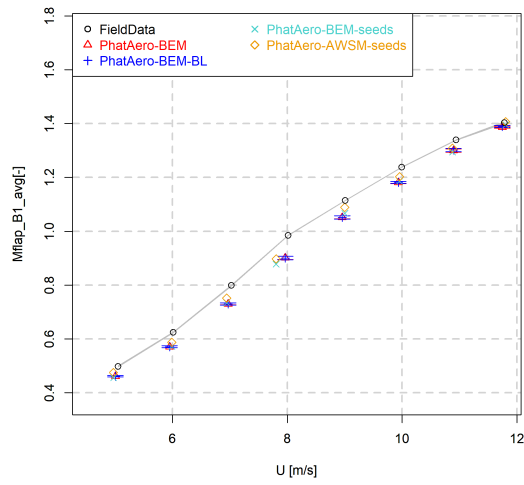
(d) Pitch angle stdev blade 1



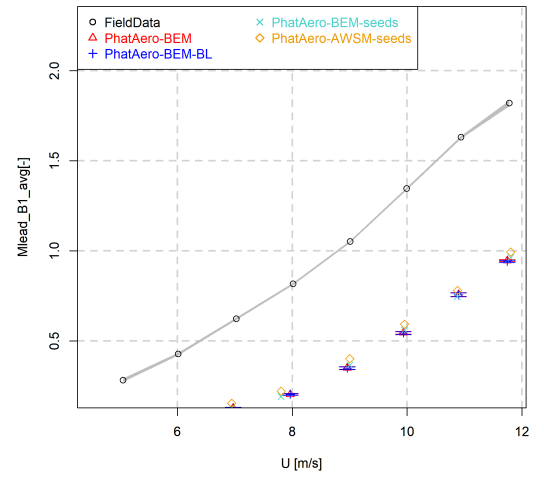
(e) Yaw misalignment



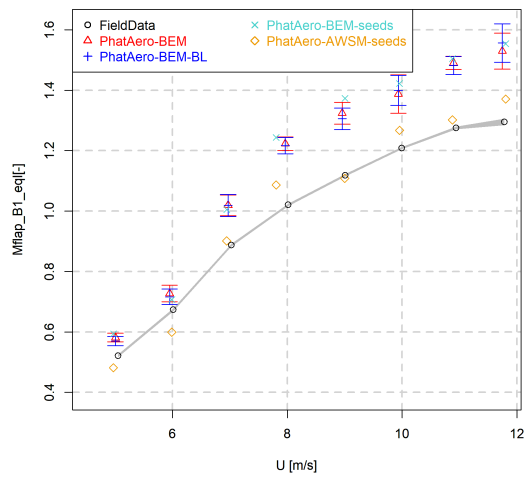
(f) Generator power (values non-dimensionalized using the average of the field data results over all wind speed bins)



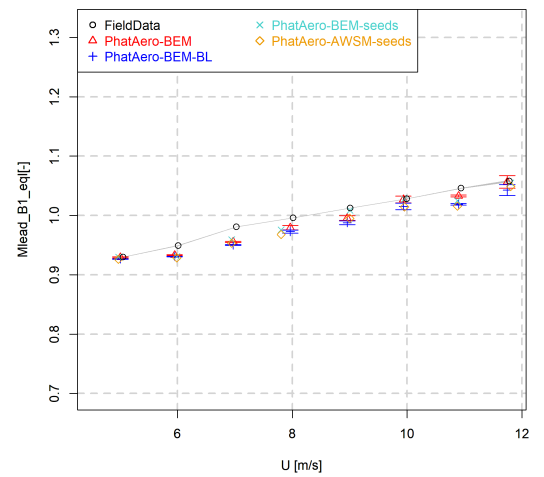
(a) Flatwise moment avg blade 1



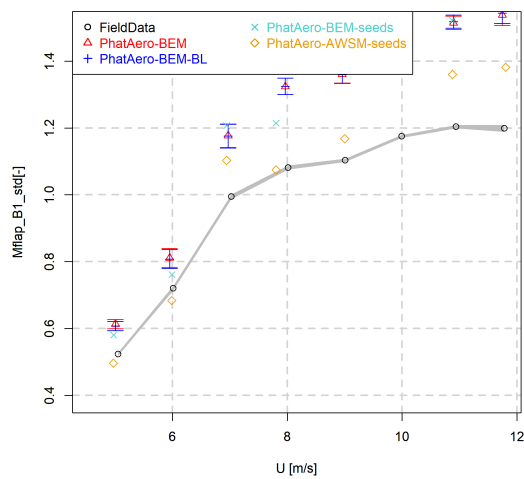
(b) Edgewise moment avg blade 1



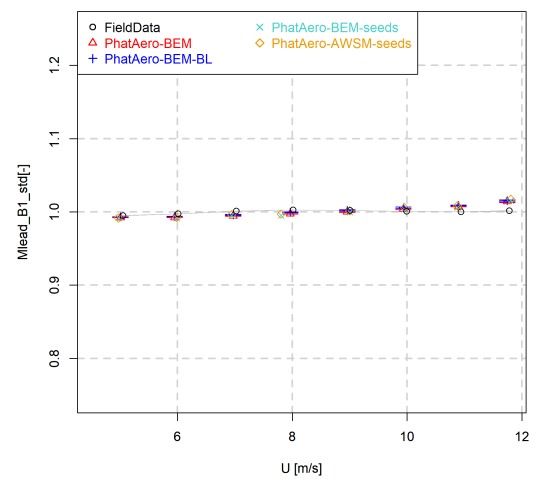
(c) Flatwise moment eq1 blade 1



(d) Edgewise moment eq1 blade 1

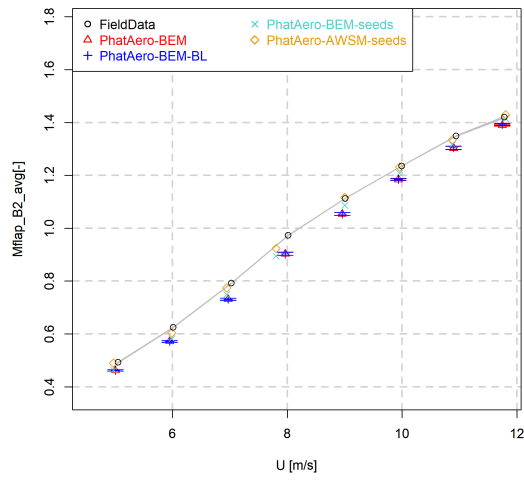


(e) Flatwise moment std blade 1

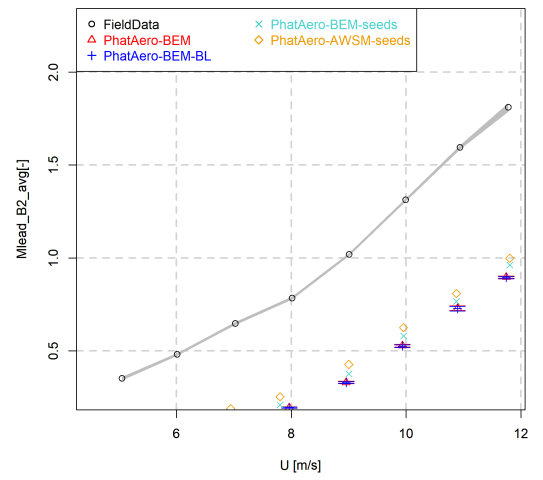


(f) Edgewise moment std blade 1

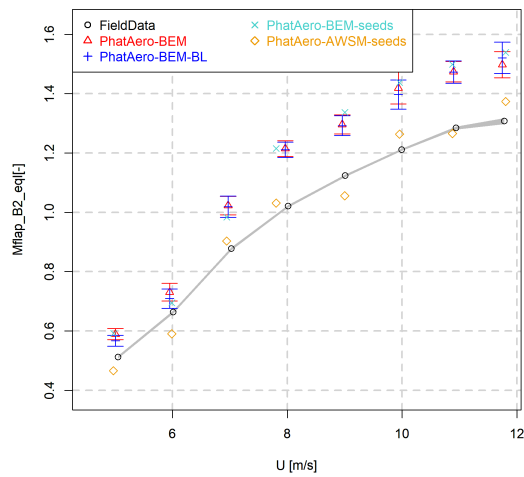
Figure D.2: Comparison between field data and simulations. All values are non-dimensionalized using the average of the field data results over all wind speed bins



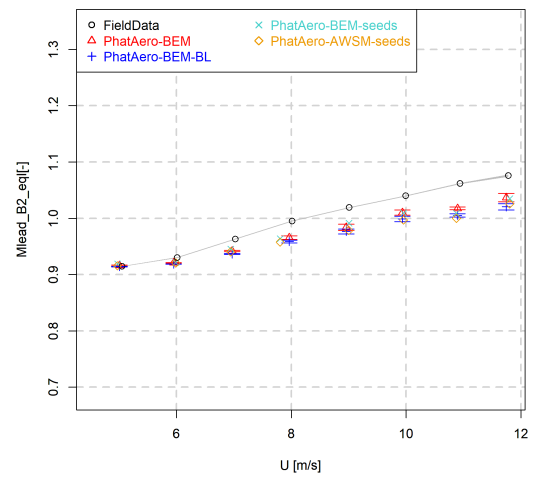
(a) Flatwise moment avg blade 2



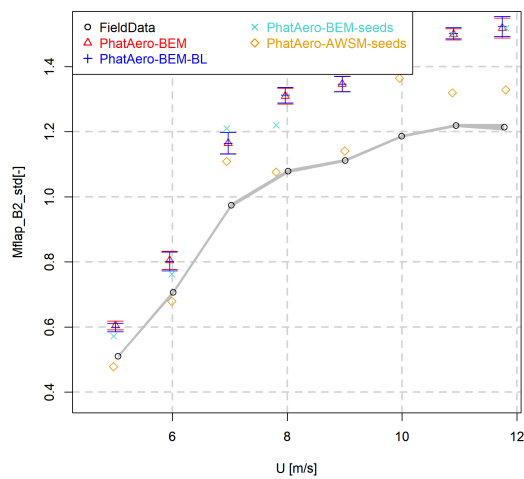
(b) Edgewise moment avg blade 2



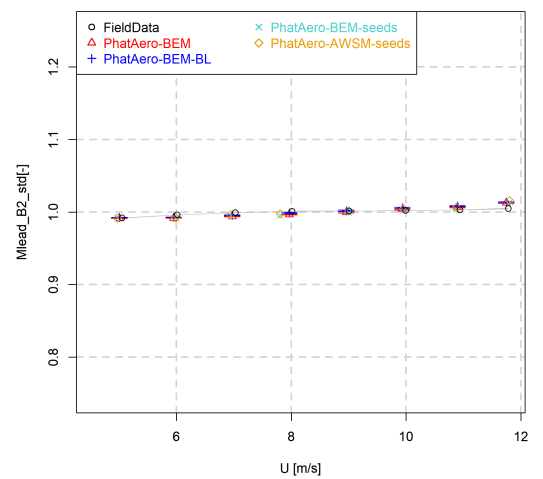
(c) Flatwise moment eq1 blade 2



(d) Edgewise moment eq1 blade 2

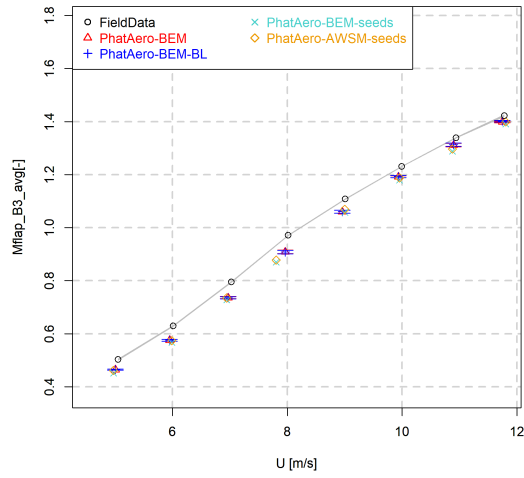


(e) Flatwise moment std blade 2

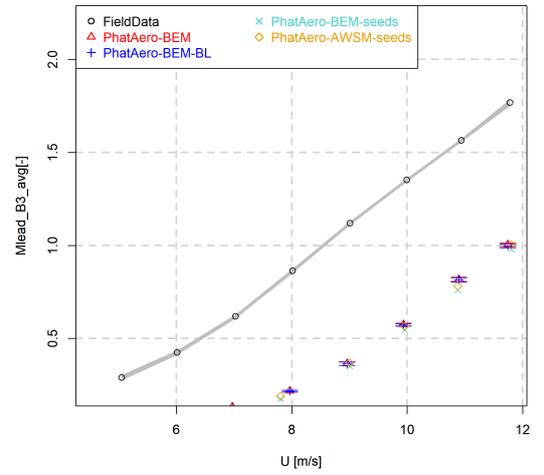


(f) Edgewise moment std blade 2

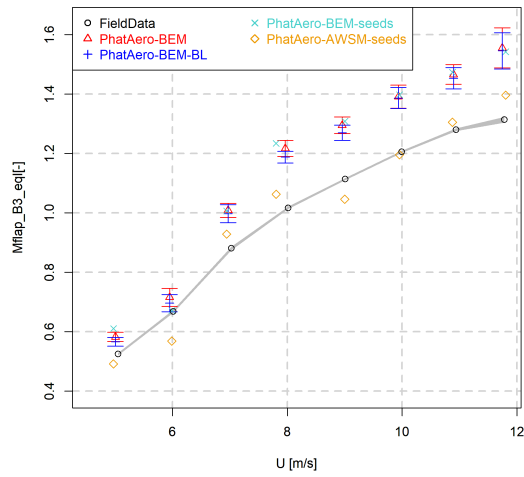
Figure D.3: Comparison between field data and simulations. All values are non-dimensionalized using the average of the field data results over all wind speed bins



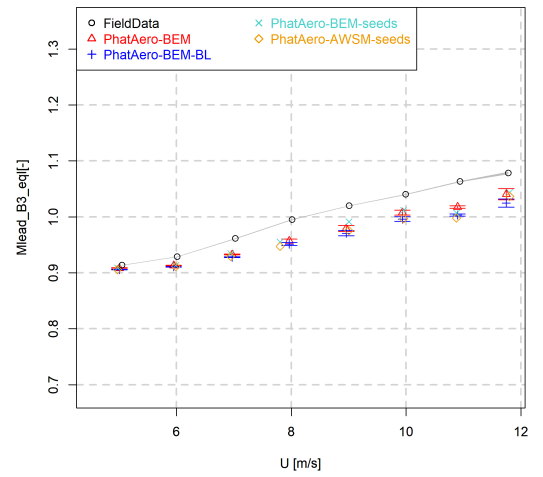
(a) Flatwise moment avg blade 3



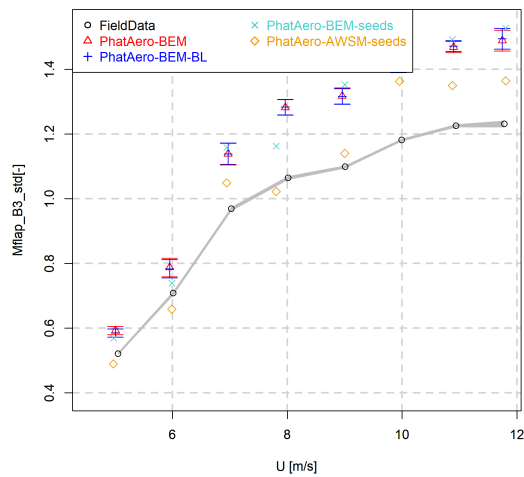
(b) Edgewise moment avg blade 3



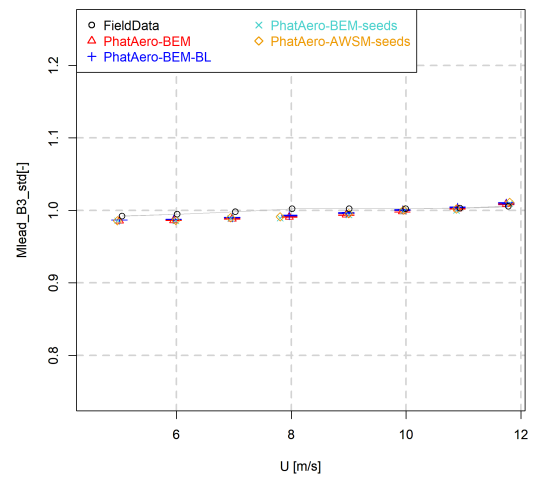
(c) Flatwise moment eq1 blade 3



(d) Edgewise moment eq1 blade 3



(e) Flatwise moment std blade 3



(f) Edgewise moment std blade 3

Figure D.4: Comparison between field data and simulations. All values are non-dimensionalized using the average of the field data results over all wind speed bins